

THREE-DIMENSIONAL IMAGING OF TURBULENT FLOWS

Rahul R. Prasad and K.R. Sreenivasan

Mason Laboratory, Yale University, New Haven, CT 06520

ABSTRACT

The three-dimensional turbulent field of a passive scalar has been mapped quantitatively by obtaining, effectively instantaneously, several closely-spaced parallel two-dimensional images. The two-dimensional images themselves have been obtained by the laser-induced fluorescence technique. Turbulent jets and wakes in water at moderate Reynolds numbers are used as examples. The spatial resolution of the measurements is about two to three Kolmogorov scales. The first contribution of this work concerns the three-dimensional nature of the boundary of the scalar-marked regions (the 'scalar interface'). It is concluded that interface regions detached from the main body are exceptional occurrences (if at all), and that in spite of the large structure, the randomness associated with small scale convolutions of the interface are strong enough that any two intersections of it by parallel planes are essentially uncorrelated even if the separation distances are of the order of a few Kolmogorov scales. The fractal dimension of the interface is determined directly by box-counting in three dimensions, and the value of 2.35 ± 0.04 is shown to be in agreement with that previously inferred from two-dimensional sections. This justifies the use of the method of intersections. The second contribution involves the simultaneous measurement of all three components of the quantity χ^* , the appropriate approximation to the scalar 'dissipation'.

1. INTRODUCTION

A capability to map quantitatively the turbulent velocity and/or passive scalar fields in three-dimensional space would be of immense value in understanding the dynamics as well as the topology of spatial structures. The issues that can be settled by such efforts are both basic and practical, and we assume that it is not necessary to dwell on them at any great length. Some examples are the three-dimensional nature of the interface bounding the vortical or scalar-marked regions, the joint statistics of the scalar concentration and its dissipation rate (of interest in fast chemistry reactions), the scaling relations of energy and scalar dissipation fields, issues relating to local isotropy, coherent structures, etc. Here, we describe a technique for mapping quantitatively the three-dimensional field of a passive scalar, and present results concerning several aspects associated with it.

The technique consists of obtaining several closely-spaced parallel two-dimensional images essentially instantaneously, and reconstructing the three-dimensional field on the computer using appropriate reconstruction algorithms. Two-dimensional images are obtained by the laser induced fluorescence (LIF) technique. LIF involves doping the turbulent flow of interest by a fluorescent dye, inducing fluorescence by illuminating it with a thin sheet of laser light, and capturing the fluorescence radiation

on to a digital camera. Several such two-dimensional images are obtained in rapid succession by sweeping the laser sheet through the flow field. The succession of two-dimensional images is captured *quantitatively* on an array of charge-coupled-devices (CCD) using a framing camera capable of operating at the rate of 10^4 frames per second. The time lapse during the entire sequence is small enough that effectively no fluid motion occurs even on the smallest dynamical scale.

In the past, single 'point' measurements of the three components of the scalar dissipation have been measurements by using a combination of cold wires (e.g., Sreenivasan, Antonia & Danh 1977). In recent years, several research groups (Agui & Hesselink 1987, Yip, Fourchette & Long 1986, Kychakoff et al. 1987) have taken advantage of the repeatability of the large structure in externally driven flows, and have obtained similar three-dimensional field of the scalar and flow fields. So far as we are aware, the only previous successful effort similar in scope to the present (namely the quantitative mapping of the passive scalar field in naturally developing turbulent flows) is due to Yip et al. (1987) and Yip (1988). These authors essentially developed the present technique and used it in gas jets seeded with Mie-scattering particles. We use the LIF technique instead of Mie-scattering, and work at moderate Reynolds numbers water jets. It is unfortunate that Yip's measurements had difficulties in matching pixel positions in nearby parallel images, which made it difficult to extract quantitative information concerning the derivatives of the scalar field. In the present measurements, this difficulty has been surmounted as described in section 3.

The present measurements have been made in round jets and wakes behind circular cylinders, both generated at moderately large Reynolds numbers; the working fluid is water. A quantity of interest is the three-dimensional nature of the boundary marking the scalar-marked regions. Another quantity concerns (an approximation to) the dissipation field of the scalar concentration. Historically, such flow properties have been measured using point probes. When the Schmidt number Sc is unity or smaller (the Schmidt number being the ratio of the kinematic viscosity to the mass diffusivity of the scalar), the temporal characteristics of these measurements is excellent (good resolution, large record lengths) but the spatial information they yield is limited. Two dimensional LIF images in the recent past have provided useful information in a plane. By the present technique, on the other hand, we obtain information in three-dimensional space.

The best spatial resolution attained in the present experiments is about 3η , where the Kolmogorov scale η represents the smallest dynamically relevant scale. For passive scalars with $Sc \gg 1$, the appropriate smallest scale is the Batchelor scale $\eta_b = \eta Sc^{-1/2}$ (Batchelor 1959). The fluorescing

dye (sodium fluorescein) has a Schmidt number of about 1900 (see Ware et al. 1983), and so the Batchelor scale is much smaller than the best resolution attained here. The essential point is that, in spite of this limitation, the present measurements will enable us to assess the *scaling properties* of the scalar dissipation structure in the inertial-convective range. We can also make qualitative statements about aspects such as the connectivity in three dimensions of the scalar-marked regions or the contiguity or otherwise of the interface. (We must make the obvious cautionary note that the scalar-marked regions do not necessarily correspond to regions containing turbulent vorticity.) We can further obtain the fractal dimension of the interface directly by box-counting in three dimensions without invoking the additive laws (see Sreenivasan & Meneveau 1986, Sreenivasan, et al. 1989) that one should use to interpret measurements in lower dimensional subspaces.

By experimental techniques such as the present, or by direct numerical solution on a massive computer of the governing equations, it is now relatively easy to generate large amounts of data in a short time. One of the pertinent questions in turbulence research today is to sort out the data in a way that can be comprehended relatively easily. We have already addressed this issue in the context of two-dimensional images, for which we obtained the so-called generalized dimensions and the singularity spectra. The significance of these quantities, without going into too many details here, is the following. In statistical mechanics, first order information is carried by the thermodynamic quantities such as temperature, internal energy, entropy, free energy, etc. If we treat a given turbulent field as a statistical mechanical system (in the sense explained in Chhabra, Jensen & Sreenivasan, 1989), the generalized dimensions and the singularity spectra correspond to such thermodynamic quantities. Using the three-dimensional images we have computed such singularity spectra. For lack of space here, we report details elsewhere (Prasad & Sreenivasan, 1989a).

2. FLOW FACILITIES

Two fully developed turbulent flows were studied. The wake behind a circular cylinder was produced by lowering a tank of water past a rigidly mounted cylinder. The cylinder used was 1 cm in diameter and had an aspect ratio of 58. The tank was lowered at a constant speed of 15 cm/s by means of a hydraulic lift. The reason that the tank, rather than the cylinder, was moved is that the water-filled tank, being much more massive than the cylinder, vibrates far less. The fluorescent dye (sodium fluorescein) that seeped into the wake from a narrow channel cut along the length of the cylinder – either at the front or the back stagnation regions – was mixed by the turbulence in the wake. These dye-marked regions were imaged and analyzed.

The axisymmetric jet was produced by allowing water to flow from a settling chamber through a nozzle of circular cross-section into a tank of still water at a constant speed of about 35 cm/s. The nozzle (diameter 1.2 cm) was contoured according a fifth order polynomial to have zero slopes and curvature at the entrance and the exit. The contraction ratio was about 10. It was established by running separate air experiments that there were no internal separations in the nozzle. The water that issued from the nozzle was dyed with the fluorescent dye. Again, the flow regions marked by the dye were imaged.

3. EXPERIMENTAL TECHNIQUES

Since the basic experimental technique involves obtaining several parallel two-dimensional sections, details described in another paper (Prasad & Sreenivasan 1989b) are relevant, and the reader is referred to it. Here, only a brief summary of those aspects are provided. Additional details involved in three dimensional imaging are described here.

In both flows the dye concentration was mapped

quantitatively using the LIF technique. Fluorescence was excited in the dye by illuminating the flow with a pulsed sheet of laser radiation. When the fluorescence is not saturated, the fluorescence intensity is directly proportional to the concentration of fluorescent dye. Care was taken to ensure that this was indeed the case in the present experiments. When fluorescence radiation from a single laser pulse (pulse duration shorter in duration than any of the characteristic time scales in the flow) is imaged on to a digital camera, a quantitative map of the instantaneous concentration of the dye in a plane is obtained. If, however, instead of using a pulsed laser, a continuous sheet of laser radiation sweeping through the flow is used in conjunction with a camera having fast enough shutter speed and high enough repetition rate, several parallel instantaneous two-dimensional maps of the concentration field could be simultaneously obtained. If these planes are sufficiently close to each other one can reconstruct the three-dimensional field on a computer.

A schematic of the experimental arrangement is shown in figure 1. The beam from an Argon ion laser was guided to the flow field using the two mirrors labeled M and RM. The circular beam from the laser was converted to a sheet approximately 200 μm thick by a combination of two lenses L, one cylindrical (focal length = 25.4 mm) and another spherical (focal length = 1000 mm). The fluorescence excited by the laser radiation was imaged by the framing camera FC, capable of acquiring a sequence of up to 16 frames at a rate of 10^4 frames/sec. The images captured by the framing camera are then digitized and stored by the CCD camera (labeled CCD in the figure). The CCD camera has a large format CCD chip with an array of 1320×1035 pixels. The digital data were then transferred to a VAXstation II/GPX computer on which all further processing was done.

The flow seeded with the fluorescent dye was created in the tank; the figure shows the cylinder C used for the wake experiments. The sheet of laser radiation was swept through the flow field using the rotating mirror RM. At different discrete times, the sheet of light produces LIF in different planes. The goal is to capture the LIF in these planes successively at a fast enough rate. Given the framing rate of the camera, the speed of

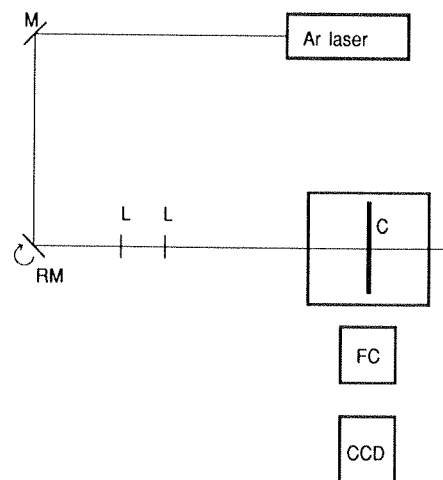


Figure 1: Schematic of the experimental apparatus used for three-dimensional imaging. Shown is the orientation of the cylinder whose wake is the object of imaging here. The continuous Argon laser has an output of 6 Watts.

the rotating mirror was adjusted to yield an interplane distance of 500 μm . The rotating mirror was 140 cm away from the region of the flow field imaged. This distance is very large compared to the interplane distance so that any two adjacent sheets of laser radiation can be regarded as parallel.

While in essence the scheme is simple, the technique is made possible only because of the speed at which the framing camera can acquire images. The exposure time for each image is 20 μs (which is negligibly small compared to all relevant time scales in the flow) and the interframe period is 80 μs . Thus the overall time required to capture the sequence of 8 parallel two-dimensional images is 800 μs . This time is also tolerably small compared to the time scales of interest in the flow, enabling an effectively instantaneous measure to be obtained of the concentration field in three dimensions.

It is important to comment a little more on the details of the image acquisition procedure. The framing camera writes, in sequence, each of the images it acquires on a phosphor screen. This phosphor screen, which contains all the images acquired by the framing camera, is then imaged by the CCD camera. Thus a single frame of the CCD camera acquires all eight frames captured by the framing camera. This imposes a limitation on the spatial extent of each of the images. Also the resolution of the images is limited to the resolution of the phosphor screen, which was 7 line pairs per mm (i.e., the closest pair of lines that can be distinguished are 75 μm apart on the phosphor screen). Since the normal image reduction ratios used in the experiments are 6, this limits the spatial resolution to 450 μm . This is also the rationale for adjusting the speed of the rotating mirror to yield an interframe separation of about 500 μm .

To ensure high quality images with good signal to noise ratios, each sequence of parallel planes was acquired using a fresh tank of filtered water. Background noise due to dark noise in the CCD camera is also subtracted from the images. Non-uniformities due to the laser sheet and optical components in the system were also corrected for (see Prasad & Sreenivasan, 1989a for details).

The wake behind a circular cylinder was created at a moderate Reynolds number of 1500 (based on the cylinder diameter and the free stream relative speed). The smallest dynamical scale, the Kolmogorov scale η , was estimated to be about 160 μm . Since the Schmidt number Sc of the dye is rather high, scales down to the Batchelor scale $\eta_b \sim \eta Sc^{-1/2}$ do exist. However, it has been argued (Sreenivasan, Ramshankar & Meneveau, 1989) that the scaling properties in the scale range above η can be considered without necessarily having to resolve scales between η_b and η ; more recent measurements to be discussed in detail elsewhere, confirm this conclusion. This feature permits us to concentrate on the scale-similar properties above the Kolmogorov scale. Each image of the wake extends approximately from 70 to 80 diameters downstream of the cylinder. As already remarked, each pixel has an area resolution of about 500 $\mu\text{m} \times 500 \mu\text{m}$, and the distance between any two parallel images was arranged (by adjusting the speed of the rotating mirror) to be about 500 μm , so that quantitative data on the concentration field is available on a three-dimensional grid of 500 μm on the side. In dynamical terms, this resolution translates to about 3 Kolmogorov scales. So far, we have worked with eight parallel planes, each 175 pixels \times 150 pixels in extent, but we are currently in the process of doubling the number of parallel planes.

A typical experimental run proceeds as follows. The tank is filled with filtered water and raised using a hydraulic lift such that the circular cylinder is close to the bottom of the tank. The dye is then allowed to flow from the slit cut along the lower end of the cylinder and the tank is lowered at the desired speed producing the wake. As the tank drops the wake is illuminated by the rotating laser beam. When the bottom of the tank recedes

to about 120 diameters downstream of the cylinder the shutters of the framing camera and the CCD camera are opened. A photodiode then detects the presence of the laser sheet in the region being imaged and triggers the electronics in the framing camera that acquires the images. Figure 2 shows the concentration field on a typical set of eight parallel planes. Also shown, in white, is the interface (to be discussed below).

The procedure followed to image the axisymmetric jet was essentially the same as that used for the wakes. In the case of the jet the Reynolds number based on nozzle diameter and velocity (~ 4000) is somewhat higher, but still only moderately high. The region imaged in the jet extended from 13 to 21 diameters downstream of the nozzle. The pixel resolution as well as the

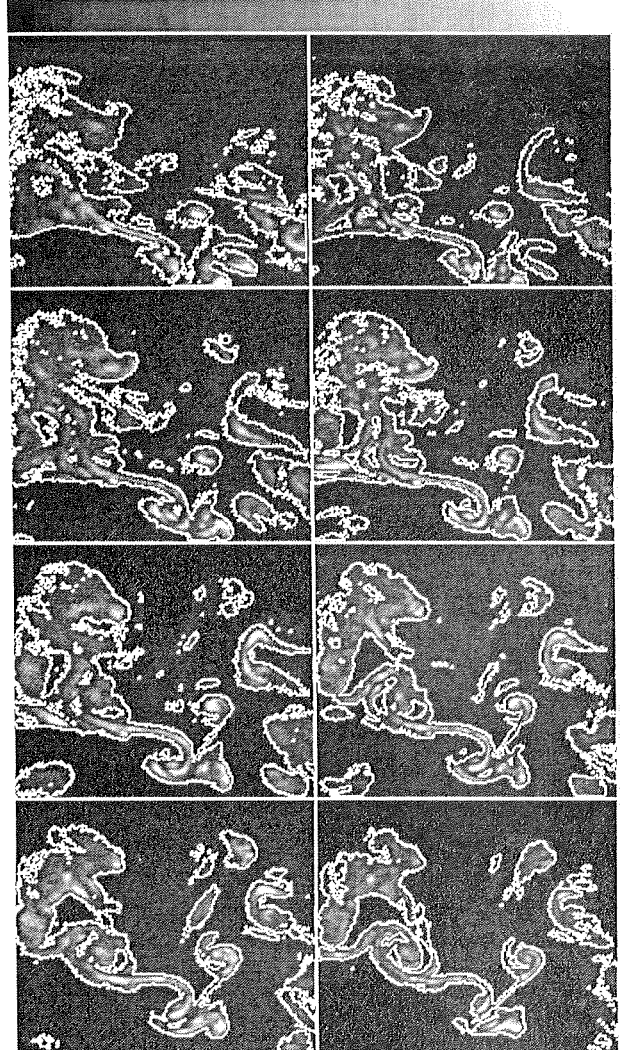


Figure 2: Concentration field of scalar-marked regions of a turbulent wake behind a circular cylinder in a set of eight parallel planes. The flow moves from left to right in each of the eight planes. The plane farthest from the cameras is the plane in the bottom right corner of the image. As one moves from right to left in the figure and then from bottom to top the planes move closer to the cameras. Also shown (in white) is the computer generated curve bounding the scalar-marked regions in the wake.

sheet thickness remain the same, and so quantitative data on the concentration field is available (as before) on a grid 500 μm on the side. This resolution is also about 2 or 3 Kolmogorov scales. Again eight parallel planes are acquired as in the wake experiments. Figure 3 shows a typical set of eight parallel planes, each displaying the concentration of the scalar-marked regions.

A critical element of quantitative data analysis is the integrity of data. This is established here in two ways. First, a number of *a priori* considerations were given to enhance the quality of data acquisition. Second, comparisons were made as appropriate with previous data of known accuracy. Some of these data are obtained by standard point probes (such as cold wires in heated flows), but some of the present data have no analogues in such point measurements. In the latter cases, we have made

comparisons with our own earlier data in which the entire CCD array was used to acquire single images. The details of these comparisons have been presented elsewhere (Prasad & Sreenivasan, 1989a).

We now have several parallel two-dimensional images. To obtain a composite three-dimensional image, it is necessary to make a perfect pixel match between two parallel images. This becomes especially important for obtaining concentration gradients in the z-direction, i.e., the direction in which the laser sheet rotates. To do this, a stationary object such as a meter scale or a stationary blob of dye in the plane of the visualization was imaged using the framing and CCD camera setup. Each of the eight images of the sequence was first roughly cut and overlaid in pairs of two, taking the difference in intensity. The images were then moved around with respect to each other to minimize the difference in intensity. This minimum occurs only when the successive images have a perfect pixel matching. Subsequent sequences of parallel planes can then all be aligned correctly; the difference in pixel intensity between two parallel planes gives a correct measure of the z-gradient of the concentration fluctuations.

4. THE GEOMETRY OF THE SCALAR INTERFACE

An interface of primary interest in the study of turbulence is that separating regions of intense and zero vorticity; another important interface is that separating the scalar-marked regions of the flow from the remaining (the 'scalar interface'). From the images acquired here, one can examine several features of the scalar interface. Elsewhere (Prasad & Sreenivasan 1989c) we have discussed several methods of marking this interface, but the simplest – and for the present purposes quite adequate – procedure involves setting an appropriate threshold on pixel intensity. Figure 2 shows the interface determined in each of the planes in a three-dimensional sequence of wake images (marked in white). It is obvious that the interface is highly convoluted and three-dimensional. We now turn to its characterization.

One obvious manifestation of the interface, namely the intermittency factor, has been measured by many workers starting with Townsend (1948), Corrsin & Kistler (1955) and Klebanoff (1955). As defined originally, the intermittency factor defines the fraction of time that a point probe resides in the turbulent region as the turbulent structures convect past it. From two-dimensional images we can obtain a corresponding quantity by scanning several lines perpendicular to the jet axis and determining the number of pixels which are within the scalar-mixed region. Details of these observations have been presented elsewhere (Prasad & Sreenivasan, 1989a).

A two-dimensional section of the flow such as the bottom right (farthest from the camera) frame in figure 3 show some scalar-marked regions that are apparently detached from the main body of the flow (for example the one marked D in the figure). It is conceivable that this part is not really detached at all but is contiguous with the main body through an out-of-plane connection. The connection to the main jet is clearly established in the fourth image in the sequence (second from the bottom in the left column). The wake images have similar occurrences also, but cases seem to exist where one may imagine isolated regions that appear and disappear within the sequence, leading to the potential conclusion that isolated patches do occur. But our informed judgement from the examination of several sequences is that out-of-plane connections are plausible outside of the range of the images. It appears safe to conclude that extensive disconnected regions do not exist.

A glance at the sequence of images in figures 2 and 3 shows that the large structure present in the interface persists from one parallel plane to next. However, the small structure is different. These small scale variations are in fact so prevalent that any two neighboring sections of the interface have very little correlation

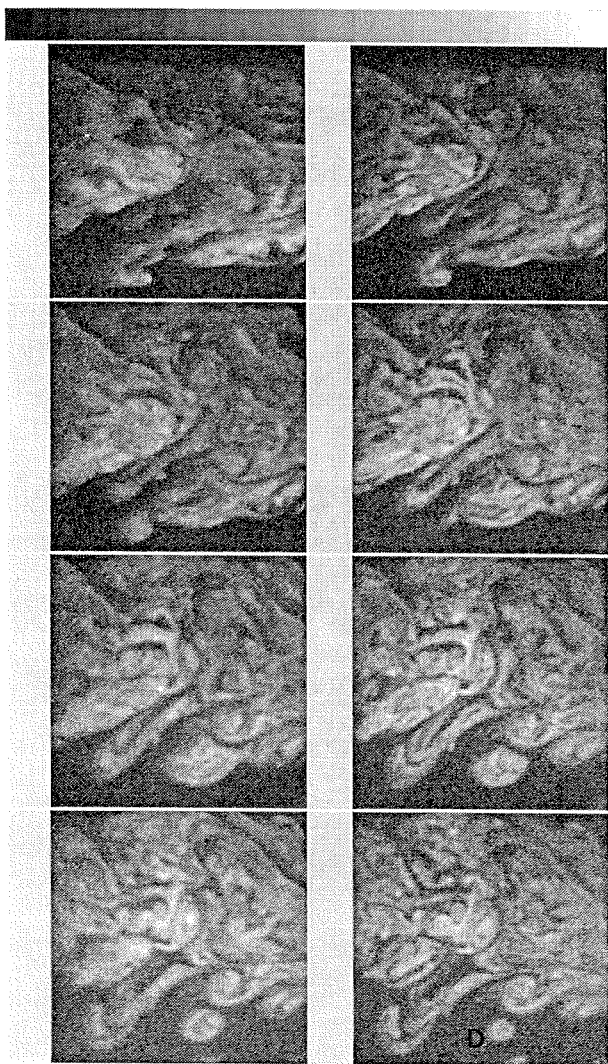


Figure 3: Concentration field of scalar-marked regions of a turbulent axisymmetric jet in a set of eight parallel planes. The flow moves from left to right in each of the eight planes. The plane farthest from the cameras is the plane in the bottom right corner of the image. As one moves from right to left in the figure and then from bottom to top the planes move closer to the cameras.

on the average. This can be quantified by defining a statistical correlation coefficient using a method based on the slope of the interface as described in Prasad & Sreenivasan (1989a). Even in adjacent frames, separated by no more than about three Kolmogorov scales, the interfaces are essentially uncorrelated; increase in the interframe distance monotonically reduces this small correlation even further. Similar calculations can be done to quantify interface correlations at larger scales by considering boxes of size larger than 4 pixels considered here. Because this operation amounts to coarse graining over small scales, it is expected that the correlation improves with the box size.

It has been shown that the interface is a fractal-like surface (Sreenivasan & Meneveau 1986); a quantity that characterizes a fractal being its fractal dimension, its measurement is of interest. The meaning of the fractal dimension and its usefulness in the contexts of mixing and entrainment are discussed in Sreenivasan, Ramshankar & Meneveau (1989). We must also remark, in view of our evidence that the interface is largely contiguous, that the fractal dimension is largely a measure of the degree of convolutedness (and not of fragmentation).

The determination of the fractal dimension of the interface (an object residing in three-dimensional space in a complex way) by the direct procedure of covering them by boxes of varying sizes is most often not practicable. We have shown elsewhere (eg. Sreenivasan & Meneveau 1986) that one way of measuring the fractal dimension of such surfaces is to measure the dimension D_s of the boundary of its intersection by a thin plane, and use the so-called law of additive co-dimensions (Marstrand 1954, Mandelbrot 1982); according to this law, the fractal dimension of the surface itself is given by D_s+1 . The fractal dimension of such two-dimensional intersections has been measured and the results presented in Sreenivasan et al. (1989). It is important to examine whether such estimates agree with that measured from the full three dimensional data. Equivalently, we want to assess directly the validity of the additive law; many indirect, but essentially complete, set of arguments were presented in Sreenivasan et al. (1989).

In our previous measurements from two-dimensional intersections, the box-counting algorithm was used to determine the fractal dimension. This algorithm (described, for example, in Sreenivasan & Meneveau 1986) basically requires that the plane of intersection (in which the boundary appears as a convoluted curve) be covered with disjoint square area elements ('boxes') of varying size. The number of boxes $N(r)$ required to cover the interface is then counted as a function of the size r of the box. If the curve is a fractal, an extended straight portion would be observed in log-log plots of $N(r)$ vs r , the negative slope of the line being the fractal dimension D_s of the boundary in intersection. Log-log plots from 2D images in the three dimensional sequence show that a well-defined straight line exists, and gives a D_s of 1.35 ± 0.05 . Using the additive law, the dimension of the interface is 2.35 ± 0.05 . This is in good agreement with the measured dimension of 2.36 from earlier single frame images. (Since the resolution in the present images is only about a third as good as in our earlier single frame ones, and we have shown elsewhere (Prasad 1989) that poorer resolution in general yields smaller fractal dimension estimates, a comment is useful on why the present agreement is so good. This is easily explained by making reference to figure 6 of Prasad (1989) which shows that the difference in fractal dimensions obtained with resolutions of the order η and 3η is quite negligible.)

As already remarked, we cannot access the entire interface in three dimensional space, its extent in the z -direction being limited to the range of approximately 3η to 24η . In this range it is possible to use the direct method of covering the interface with three dimensional boxes of varying sizes. The negative slope of the straight part of the log-log plots of $N(r)$ vs r would be the

fractal dimension of the surface. Figure 4 shows typical log-log plots obtained by boxing the accessible portion of the surface. The scaling in both jets and wakes extends over the entire range available; the average fractal dimension is 2.35 ± 0.04 for both jets and wakes. This agrees rather well with earlier measurements from one and two dimensional sections (Sreenivasan & Meneveau 1986, Sreenivasan et al. 1989), and the present two-dimensional intersections. In our view, this conclusively establishes the fractal nature of the interface of scalar-marked regions in turbulent flows. It also directly verifies the applicability in this case of the method of intersections.

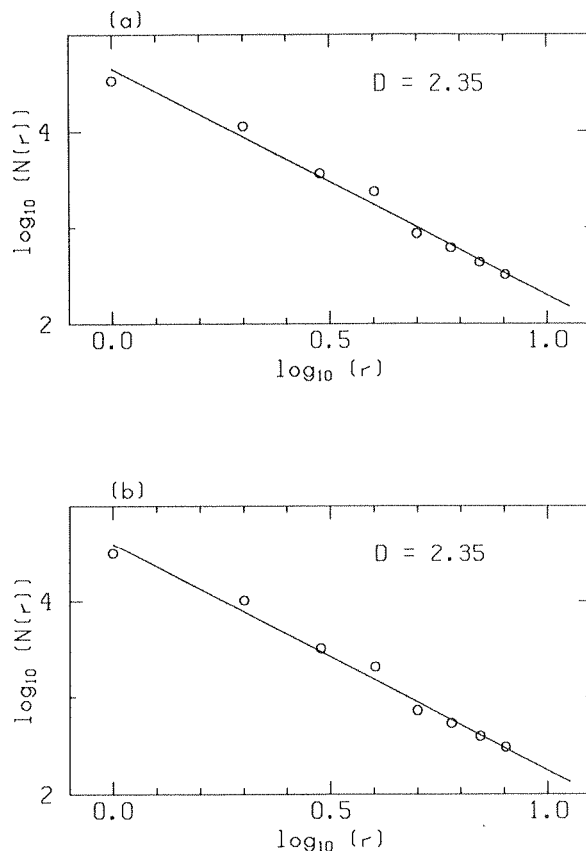


Figure 4: Typical log-log plots of the number of boxes $N(r)$ required to cover the accessible part of the interface in three dimensional space vs the size of the box r . (a) Data from the turbulent wake behind a circular cylinder. (b) Data from the axisymmetric turbulent jet. In both cases, the dimension, corresponding to the slope of the line drawn, is about 2.35.

5. SCALAR 'DISSIPATION'

A quantity of practical interest, for example in the context of turbulent mixing of reactants involving fast chemistry, is the dissipation of passive scalar fluctuations $\chi = 2\Gamma(\partial\theta/\partial x_i)^2$, where x_i represent spatial coordinates and θ is a passive scalar (e.g. concentration c of a contaminant or temperature T), and Γ the corresponding molecular diffusivity; summation is implied on the index i . This dissipation is analogous to the dissipation of turbulent kinetic energy, ϵ , but yet is different in that it does not involve cross terms and contains only three positive definite

terms. All of them can in principle be obtained by the techniques used here. Since the resolution here is between two and three Kolmogorov scales, we obtain the quantity χ^* , where

$$\chi^* = [(\Delta c)/\Delta x_i]^2, \quad (4.1)$$

and the difference concentration Δc can be obtained accurately only on scales of the order of η . For convenience, we have omitted the constant factor 2Γ in (4.1), and shall refer below to χ^* as the 'dissipation'. It is found that the 'dissipation' field is highly intermittent and the three components, while alike in the overall sense, have some differences. The details of the quantitative results concerning χ^* , the probability densities and moments of each of the 3 components of χ^* and the joint probability density of χ^* and c have been presented elsewhere (Prasad & Sreenivasan, 1989a).

A fundamental aspect of the dissipation field is its spatial and temporal intermittency. It is clear that such highly intermittent processes cannot be described efficiently by conventional moment methods which are good for Central Limit type processes; in particular, if the process is Gaussian, its mean and variance describe the process completely. It has been recognized (Mandelbrot 1974, Frisch & Parisi 1985, and Halsey et al. 1986, Meneveau & Sreenivasan, 1987) that intermittent measures arising in nonlinear systems lend themselves to be characterized by what are called multifractals in the present parlance of dynamical systems. In this picture, local singularities of different strengths α are distributed on interwoven sets of varying dimensionality $f(\alpha)$. Such a singularity spectrum has been obtained and the results presented elsewhere (Prasad & Sreenivasan, 1989a).

6. SUMMARY

We have measured the three dimensional field of a passive scalar in fully turbulent flows. The technique consists in the quantitative mapping, effectively instantaneously, of the concentration field in several parallel planes. This is made possible by combining the unique capabilities of the framing camera with a relatively large CCD array. The measurements allow us to examine several issues concerning the three dimensional structure of the passive scalar field. First, several aspects of the scalar interface have been studied. We showed that the scalar-marked regions do not generally detach themselves from the main body. We then devised a simple scheme for correlating the interface shape from one parallel plane to another. Its application showed that in spite of the large structure, the randomness associated with small scale convolutions of the interface are strong enough that any two intersections of it by parallel planes are essentially uncorrelated even if the separation distances are of the order of a few Kolmogorov scales. The fractal dimension of the interface was determined directly by box-counting in three dimensions, and the value of 2.35 ± 0.04 is shown to be in agreement with that previously inferred from two-dimensional sections. This justifies the use of the method of intersections.

We have also established the quality of the data by making, where possible, comparisons with previous measurements. Although the resolution in the present measurements is on the order of three Kolmogorov scales, it is believed that most of the conclusions are generally sound qualitatively. In particular, the scaling properties in the appropriate scaling range are believed to be correct.

Another contribution has been the measurement, simultaneously, of all three components of the scalar 'dissipation' field. The quantitative information that is obtained as a result of these measurements is presented elsewhere.

ACKNOWLEDGEMENT

We gratefully acknowledge the financial assistance from a DARPA (URI) grant and an instrumentation grant from AFOSR.

REFERENCES

- Agui, J.C. & Hesselink, L. 1987 *J. Fluid Mech.*
 Batchelor, G.K. 1959 *J. Fluid. Mech.* **5**, 113.
 Chhabra, A., Jensen, R.V. & Sreenivasan, K.R. 1989 *Phys. Rev. A* (in print).
 Corrsin, S. & Kistler, A. L. 1955 *NACA Rep.* 1244
 Frisch, U. & Parisi, G. 1985 In *Turbulence and Predictability in Geophysical Fluid Dynamics and Climate Dynamics* (ed. M. Ghil, R. Benzi & G. Parisi) p. 84, North-Holland.
 Halsey, T.C., Jensen, M.H., Kadanoff, L.P., Procaccia, I. & Shraiman, B.I. 1986 *Phys. Rev.* **A33**, 1141.
 Klebanoff, P.S. 1955 *NACA Rep.* 1247.
 Kychakoff, G., Paul, P.H., van Cruyningen, I. & Hanson, R.K. 1987 *Appl. Optics* **26**, 2498.
 Mandelbrot, B.B. 1974 *J. Fluid Mech.* **62**, 331.
 Mandelbrot, B.B. 1982 *The Fractal Geometry of Nature*, W.H. Freeman.
 Marstrand, J.M. 1954 *Lond. Math. Soc.* **3**, 257.
 Meneveau, C. & Sreenivasan, K.R. 1987 *Nuclear Phys. B. (Proc. Suppl.)* **2**, 49.
 Prasad, R.R. 1989 *Proceedings of the Forum on Chaotic Dynamics, ASME Fluids Engineering Spring Conference*, La Jolla, CA.
 Prasad, R.R. & Sreenivasan, K.R. 1989a Submitted to *J. Fluid. Mech.*
 Prasad, R.R. & Sreenivasan, K.R. 1989b In preparation.
 Prasad, R.R. & Sreenivasan, K.R. 1989c *Expts. in Fluids* **7**, 259.
 Sreenivasan, K.R., Antonia, R.A. & Danh, H.Q. 1977 *Phys. Fluids* **20**, 1238.
 Sreenivasan, K.R. & Meneveau, C. 1986 *J. Fluid Mech.* **173**, 357.
 Sreenivasan, K.R., Ramshankar, R. & Meneveau, C. 1989 *Proc. R. Soc. Lond.* **A421**, 79.
 Sreenivasan, K.R., Prasad, R.R., Meneveau, C. & Ramshankar, R.R. 1989 *Pure & Appl. Geophys. J.* **131** (in print)
 Townsend, A.A. 1948 *Aust. J. Sci. Res.* **2A**, 451.
 Ware, B.R. et al. 1983 In *Measurement of Suspended Particles by Quasi-Elastic Light Scattering*, ed. B.E. Dahneke, Wiley, 255.
 Yip, B., Fourgette, D.C. & Long, M.B. 1986 *Appl. Optics* **25**, 3919.
 Yip, B., Lam, J.K., Winter, M. & Long, M.B. 1987 *Science* **235**, 1209.
 Yip, B. 1988 Ph. D. thesis, Yale University.